

Article

# Photochemical Reflectance Index (PRI) for Detecting Responses of Diurnal and Seasonal Photosynthetic Activity to Experimental Drought and Warming in a Mediterranean Shrubland

Chao Zhang <sup>1,2,\*</sup> , Iolanda Filella <sup>1,2</sup>, Daijun Liu <sup>1,2</sup>, Romà Ogaya <sup>1,2</sup>, Joan Llusà <sup>1,2</sup>, Dolores Asensio <sup>1,2</sup> and Josep Peñuelas <sup>1,2</sup> 

<sup>1</sup> CREAM, 08193 Cerdanyola del Vallès, Catalonia, Spain; iola@creaf.uab.cat (I.F.); d.liu@creaf.uab.cat (D.L.); r.ogaya@creaf.uab.cat (R.O.); j.llusia@creaf.uab.cat (J.L.); loles@creaf.uab.cat (D.A.); josep.penuelas@uab.cat (J.P.)

<sup>2</sup> CSIC, Global Ecology Unit CREAM-CSIC-UAB, 08193 Bellaterra, Catalonia, Spain

\* Correspondence: c.zhang@creaf.uab.cat; Tel.: +34-93-5813-355

Received: 12 October 2017; Accepted: 17 November 2017; Published: 20 November 2017

**Abstract:** Climatic warming and drying are having profound impacts on terrestrial carbon cycling by altering plant physiological traits and photosynthetic processes, particularly for species in the semi-arid Mediterranean ecosystems. More effective methods of remote sensing are needed to accurately assess the physiological responses and seasonal photosynthetic activities of evergreen species to climate change. We evaluated the stand reflectance in parallel to the diurnal and seasonal changes in gas exchange, fluorescence and water contents of leaves and soil for a Mediterranean evergreen shrub, *Erica multiflora*, submitted to long-term experimental warming and drought. We also calculated a differential photochemical reflectance index ( $\Delta$ PRI, morning PRI subtracted from midday PRI) to assess the diurnal responses of photosynthesis ( $\Delta A$ ) to warming and drought. The results indicated that the PRI, but not the normalized difference vegetation index (NDVI), was able to assess the seasonal changes of photosynthesis. Changes in water index (WI) were consistent with seasonal foliar water content (WC). In the warming treatment,  $\Delta A$  value was higher than control in winter but  $\Delta$ Yield was significantly lower in both summer and autumn, demonstrating the positive effect of the warming on the photosynthesis in winter and the negative effect in summer and autumn, i.e., increased photosynthetic midday depression in summer and autumn, when temperatures were much higher than in winter. Drought treatment increased the midday depression of photosynthesis in summer. Importantly,  $\Delta$ PRI was significantly correlated with  $\Delta A$  both under warming and drought, indicating the applicability of  $\Delta$ PRI for tracking the midday depression of photosynthetic processes. Using PRI and  $\Delta$ PRI to monitor the variability in photosynthesis could provide a simple method to remotely sense photosynthetic seasonality and midday depression in response to ongoing and future environmental stresses.

**Keywords:** drought; evergreen; midday depression; photochemical reflectance index (PRI); photosynthesis; remote sensing; warming; water index (WI)

## 1. Introduction

Droughts have occurred frequently under global warming around the world [1,2], prominently disturbing terrestrial ecosystemic services and functioning, such as water cycles [3], terrestrial production [4,5], ecosystemic respiration [4], biodiversity [6] and plant survival and mortality [7,8]. Increases in climatic warming and drought projected by some global models [1,9] could profoundly affect Mediterranean ecosystems [10–13], regions highly susceptible to climate change due

to the interaction between heat and aridity. Higher temperatures in the coming decades [10,14,15] is expected to change community structure [16,17] and decrease photosynthesis [18,19] and plant growth [20–22] in Mediterranean ecosystems, and thus to affect carbon uptake by terrestrial vegetation and to alter regional carbon balances [4,23].

Plants respond to warmer and drier conditions mainly by downregulating photosynthesis due to stomatal limitation and lack of soil water [8,18,24–26] or to electron-transport limitation and Rubisco (ribulose 1,5-bisphosphate carboxylase/oxygenase) deactivation [27,28]. Such decreases in photosynthesis are accompanied by decreases in the maximum photochemical efficiency of photosystem II (PSII,  $F_V/F_M$ ) [29]. When the sinks of reducing power decrease and photosynthesis is downregulated, the increase in the dissipation of excess energy can be estimated by quantifying the de-epoxidation state of the xanthophyll-cycle pigments (violaxanthin, antheraxanthin and zeaxanthin) [29,30], in which violaxanthin is converted to zeaxanthin via the intermediate antheraxanthin, accompanied by a decrease in the pH of the thylakoid lumen [31,32]. The increase in zeaxanthin associated with reversible non-photochemical quenching (NPQ) [31] can thus be detected by the photochemical reflectance index (PRI; [33,34]) at an absorption band of 531 nm in the vegetation spectrum. PRI tracks the rapid physiological changes that are generally difficult to follow in evergreen species using indices of greenness and canopy structure, such as the normalized difference vegetation index (NDVI) [35–37].

PRI is a good indicator of the photosynthetic apparatus across functional types and spatiotemporal scales [35,38], and has detected the reactivation of photosynthesis from winter stress in evergreen species [39–41]. The effects of seasonal drought on the photosynthetic apparatus have also been detected by satellite-based PRI [42,43]. Maximum CO<sub>2</sub> assimilation has been efficiently estimated by PRI under severe drought conditions [44], and Rossini et al. [45] demonstrated that changes in PRI were correlated with water stress in maize. Photosynthetic variability induced by heat and drought is simultaneously accompanied by complex physiological and biochemical processes, which could constrain the PRI-based estimation of the photosynthetic apparatus. Carotenoid and chlorophyll pigments and structural changes to canopies have strong effects at the canopy level and seasonal scale [35,37,38,40,46]. Many studies have focused on improving PRI to decrease the influences of pigment-pool size and canopy structural change on the seasonal detection of photosynthesis using PRI [38]. Long-term studies of PRI at ecosystemic levels have increased during the last six years (e.g., [35,38]).

The use of PRI to assess the effects of warming and drought on photosynthetic activity, however, has received little attention. Filella et al. [47] reported that a low-canopy leaf area index (LAI) at the early stage of experimental warming and drought was associated with the ability of PRI to detect photosynthesis. Mänd et al. [48] detected the impact of experimental warming and drought on the photosynthetic apparatus based on the canopy PRI. Recently, a study by Zhang et al. [49] demonstrated that PRI was not only sensitive to progressive drought effects on photosynthetic activity but also tracked photosynthetic recovery after drought stress. Importantly, the differential PRI,  $\Delta$ PRI, obtained by subtracting dark-state PRI from light-exposed PRI [50–52], or by subtracting predawn PRI from midday PRI [53], can eliminate the impacts of canopy structure and foliar pigments on interpretations of PRI. Additionally, the midday depression or downregulation of photosynthesis can affect the global carbon budget [54]. Gamon et al. [55] reported that PRI depression was associated with photosynthetic downregulation in evergreen trees. These studies led to our hypothesis that a  $\Delta$ PRI obtained by subtracting morning PRI from midday PRI could be used to detect midday photosynthetic depression.

We examined the seasonality and diurnal responses of photosynthesis to long-term experimental warming and drought in an evergreen Mediterranean shrub. The optical signals of PRI and fluorescence were measured in parallel with the photosynthetic rates and water contents of leaves and soil. The primary purpose of this study was to determine the utility of canopy PRI and  $\Delta$ PRI for assessing

seasonal and diurnal photosynthetic performance. We also assessed the influences of simulated climatic warming and drought on the photosynthetic activity in a long-term experimental system.

## 2. Materials and Methods

### 2.1. Study Site and Plant Species

The study was conducted in Garraf Natural Park on the central coast of Catalonia, Spain (41°18'N, 1°49'E; 210 m a.s.l.), on a south-facing hill (13° slope). The test species, *Erica multiflora* L., is a common evergreen, short-leaved, sclerophyllous and resprouting shrub that typically grows on calcareous soils in the western Mediterranean Basin. The vegetation coverage in Garraf is ca. 70% and is dominated by *E. multiflora* and *Globularia alypum* L., each ca. 1 m high, accompanied by other Mediterranean coastal shrubs (e.g., *Dorycnium pentaphyllum* L., *Rosmarinus officinalis* L., *Ulex parviflorus* L. and *Pistacia lentiscus* L.). *E. multiflora* re-sprouts abundantly after disturbance removal of aboveground biomass from the temporary extensive stump or from external roots near the stump [56]. Dry conditions, however, can greatly decrease the productivity of *E. multiflora* [56].

### 2.2. Experimental Design and Field Sampling

Our experiment was part of an experimental system established in 1999 and consisted of nine 20-m<sup>2</sup> plots. Six of the plots were treatments representing climate change: three drought plots and three warming plots. The remaining three were untreated control plots. The drought treatment decreased the input of rainwater in spring and autumn using a transparent plastic covering the vegetation canopy operated automatically based on the rainfall (<0.3 mm) and wind (<10 m s<sup>-1</sup>), decreasing the amount of soil water by 20% [18]. The warming treatment increased the nocturnal temperature by ca. 0.6 °C and decreased the loss of heat by 64% using a reflective aluminum curtain [18], depending on the season. The curtain was retracted automatically to avoid hydrological effects during rains. See Peñuelas et al. [57] for details of the experimental sites and treatments.

The study site has a typical Mediterranean climate characterized by a pronounced three-month summer drought, a wet spring and autumn and a cool winter. The annual precipitation in the study year was 510.2 mm, and the average monthly temperature was 15.8 °C.

Two randomly chosen *E. multiflora* plants in each plot were concurrently monitored for gas exchange, parameters of chlorophyll fluorescence and optical signals. Measurements were obtained on 12–14 February, 1–3 May, 23–25 July and 29 October–1 November 2014, i.e., three plots per day and one sampling for each season. Measurements were conducted on sunny days in the morning (8:00–10:30, solar time) and at midday (11:30–14:30, solar time) at the top of the canopy in the same plants that were selected in the morning. The start times were chosen based on the changes in solar irradiance during the year. Soil water content and temperature were also measured in the morning and at midday. Foliar water content was obtained by sampling branches at the top canopy of *E. multiflora* that were healthy and fully exposed to light in the morning.

### 2.3. Environmental and Gas-Exchange Monitoring

The air temperature and precipitation were continuously monitored at an automatic meteorological station installed at the study site in 1998. The CO<sub>2</sub> assimilation rate (*A*) and stomatal conductance (*g<sub>s</sub>*) were measured using a Li-Cor LI-6400XT Portable Photosynthesis System equipped with a LI-6400-40 Leaf Chamber Fluorometer (Li-Cor, Inc., Lincoln, NE, USA) at 25 °C and a light intensity of 1000 μmol m<sup>-2</sup> s<sup>-1</sup>. Three measurements were recorded for each plant to reduce measurement error. Total leaf area for each branch was obtained from small leaves pasted together and was then estimated from a photograph of all leaves using ImageJ 1.46r (NIH, Bethesda, MD, USA). The diurnal change of photosynthesis ( $\Delta A$ ) was expressed as morning *A* subtracted from midday *A*.

#### 2.4. Soil Water Content and Temperature

Soil water content was measured using an HH2 moisture meter with an ML2x soil-moisture sensor (Delta-T Devices Ltd., Cambridge, UK). The measurements were obtained by inserting the sensor's stainless-steel cylindrical rods into the soil to a depth of 10 cm at three randomly selected locations within each plot. Soil temperature was also measured at 10 cm using a digital soil thermometer (TO 15, Jules Richard instruments, Argenteuil, France) [58].

#### 2.5. Foliar Water Content

Five branches were sampled as replicates to analyze foliar water content (WC) and retained freshness in each plot using a portable crisper. The fresh weight (FW) of the leaves was determined immediately after transport to the laboratory. The leaves were then dried in an oven at 70 °C for two days to a constant weight (dry weight, DW). WC was then calculated as:

$$WC = (FW - DW)/FW \quad (1)$$

#### 2.6. Chlorophyll Fluorescence

The maximum photochemical efficiency of PSII ( $F_V/F_M$ ) was estimated based on measurements of minimum ( $F_0$ ) and maximum ( $F_M$ ) fluorescence by a portable miniaturized pulse-amplitude-modulated photosynthesis yield analyser (MINI-PAM, Walz, Effeltrich, Germany) with a leaf-clip holder. The leaves were dark-adapted for at least 30 min with the leaf clips.

The actual photochemical efficiency of PSII (Yield) was estimated based on the measured fluorescence parameters as:

$$\text{Yield} = (F_M' - F_S)/F_M' \quad (2)$$

where  $F_S$  and  $F_M'$  are the steady-state yield of fluorescence and the maximum fluorescence yield, respectively, during full closure of the PSII center obtained by a LI-6400-40 Leaf Chamber Fluorometer (Li-Cor, Inc., Lincoln, NE, USA) in fully exposed leaves that received the maximum amount of light corresponding to that moment of the day. This measurement was conducted synchronously with gas exchange at the same environmental conditions.

The diurnal change of Yield ( $\Delta\text{Yield}$ ) was calculated by subtracting morning Yield from midday Yield.

#### 2.7. Canopy Reflectance

Ground-based canopy spectra were measured in situ using a portable field spectroradiometer (GER1500, Geophysical & Environmental Research, Spectra Vista Corp., Poughkeepsie, NY, USA). The instrument measures spectral reflectance between 268 and 1095 nm with a sampling interval from 1.5 to 2.1 nm and a 25° field of view. The reflectance was calculated after standardization by canopy irradiance using a reference spectral panel (Spectralon, Labsphere, North Sutton, NH, USA) serving as a Lambertian reflector. All spectral measurements were from a nadir view angle approximately 0.5 m above the canopy. The area measured was thus a circle with a diameter of ca. 0.58 m on the top of the canopy. Three scans were quickly recorded (around one second per record) with the integration time of 5 ms in different positions of the top canopy for each plant as replicates after measuring the white standard spectrum. Five eco-physiological indices were calculated from the reflectance data (Table 1).

**Table 1.** Description of the formulae used to derive eco-physiological indices. The variable ‘Rx’ represents the reflectance values at x nm.

Index	Formula	Reference
Photochemical Reflectance Index (PRI)	$(R531 - R570)/(R531 + R570)$	[33,34]
Normalized Difference Vegetation Index (NDVI)	$(R900 - R680)/(R900 + R680)$	[59]
Water Index (WI)	$R900/R970$	[60]
Normalized Difference Chlorophyll Index (NDCI)	$(R750 - R705)/(R750 + R705)$	[61]
Structure-Insensitive Pigment Index (SIPI)	$(R445 - R800)/(R680 - R800)$	[62]

$\Delta$ PRI was also calculated by subtracting early morning PRI from midday PRI.

## 2.8. Statistical Analysis

The seasonal variations of gas exchange,  $F_V/F_M$ , Yield and the vegetation indices were determined using one mean per stand. One mean per plot was used for soil water content and temperature and for foliar WC. We used repeated-measures analyses of variance to detect the seasonal changes of all variables and to determine the impacts of the treatments and the water status of both leaves and soil on photosynthetic seasonality. The responses of the vegetation indices to photosynthetic seasonality and the applicability of WI for assessing WC were analyzed using standardized major-axis regression to identify correlations between the variables. We compared the fitted bivariate slopes between treatments using 95% confidence intervals and the smart R package. All analyses were conducted with R version 3.2.2 (R Core Development Team, 2015).

## 3. Results

### 3.1. Climate and Soil and Foliar Water Statuses

The seasonal mean temperatures in 2014 (Figure 1) ranged between 9.7 °C in winter and 22.4 °C in summer. The summer was wet, with a total precipitation of 161.7 mm, considerably higher than in winter (66.2 mm) and spring (79.6 mm). The year 2014 was a dry spring, wet summer year, and the summer sampling date made summer results somewhat irrelevant, as they were taken only a few days after some strong rains. Soil water content and temperature clearly varied seasonally. Soil water content (Figure 2a) was higher in winter than in the other seasons and lowest in summer for all treatments. Soil temperature (Figure 2b) was lowest in winter and highest in summer and was higher at midday for each season. Foliar WC (Figure 3) differed significantly ( $p < 0.001$ ) between seasons and decreased from winter to spring and then recovered in summer and autumn. The treatments, however, had no impacts on WC.

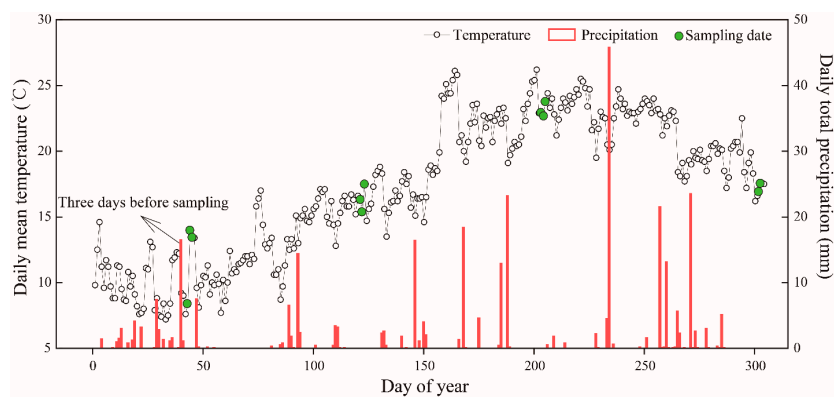


**Figure 1.** Daily mean temperature and daily total precipitation in Garraf Natural Park in 2014. Total precipitation was 66.2 mm in winter (January–March), 79.6 mm in spring (April–June), 161.7 mm in summer (July–September) and 202.3 mm in autumn (October–December). Seasonal mean temperatures were 9.7 °C (winter), 17.5 °C (spring), 22.4 °C (summer) and 13.5 °C (autumn).

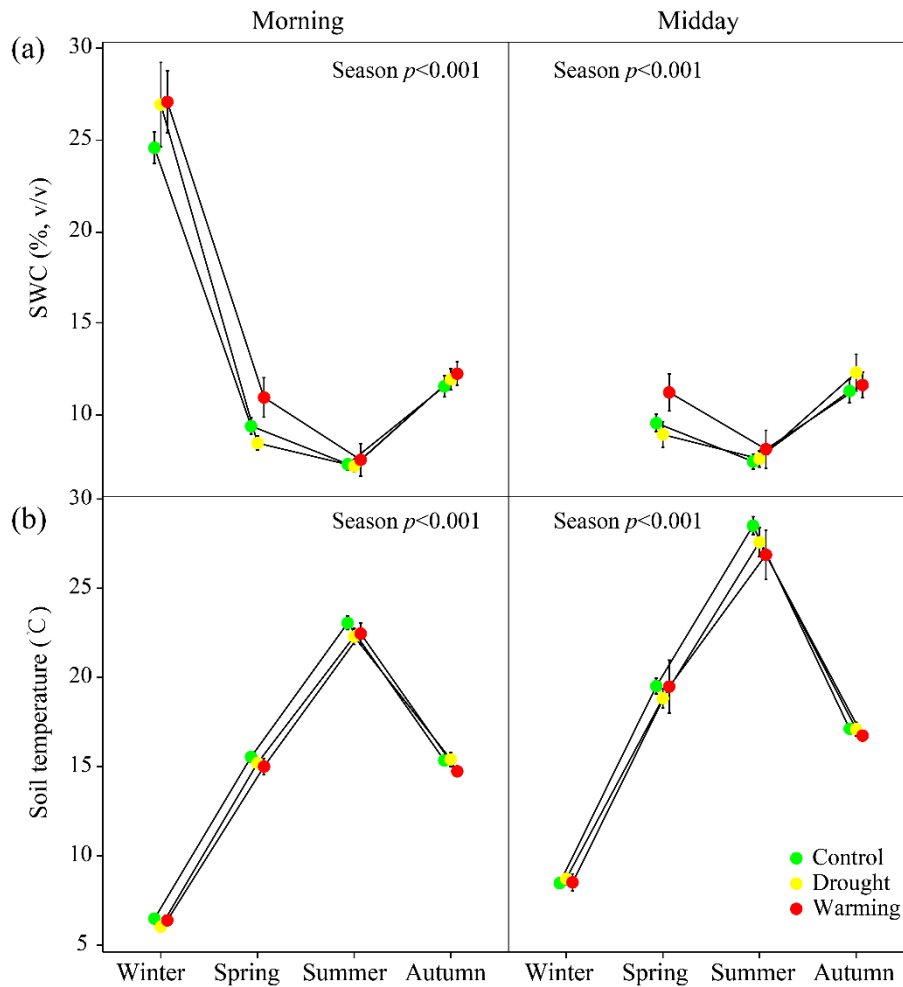


**Figure 2.** Seasonal variation of soil water content (SWC) (a) and temperature (b) in Garraf Natural Park in 2014. Error bars are standard errors of the mean (n = 9 for the drought and warming treatments, and n = 18 for the control treatment). The significances of the repeated-measures ANOVAs are depicted.

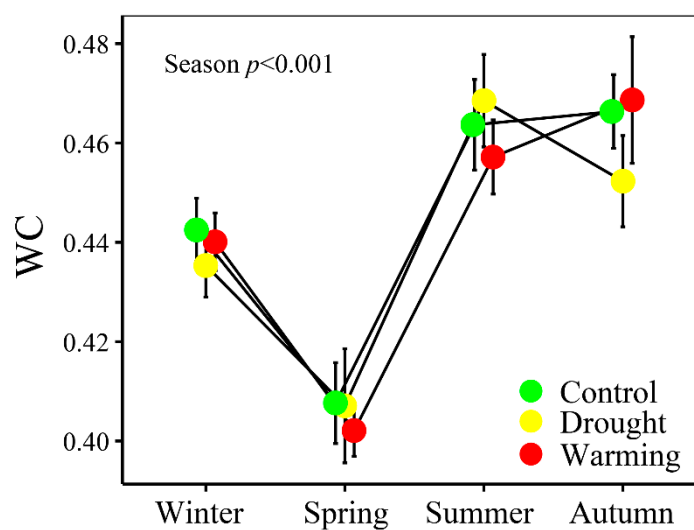


**Figure 3.** Seasonal variation of foliar water content (WC) for *Erica multiflora* in 2014. Error bars are standard errors of the mean (n = 6 for the drought and warming treatments, and n = 12 for the control treatment). The significances of overall repeated-measures ANOVAs are depicted.

### 3.2. Seasonal Patterns of Gas Exchange, Fluorescence and Vegetation Indices

The rate of CO<sub>2</sub> assimilation (*A*) (Figure 4a) was significantly lower in winter (around 2 μmol m<sup>-2</sup> s<sup>-1</sup>) than autumn (around 8 μmol m<sup>-2</sup> s<sup>-1</sup>) for both the morning and midday measurements. Midday photosynthesis was significantly lower in the drought than the control treatment throughout the year (drought < control, *p* = 0.03), particularly in autumn (*p* < 0.05). Morning stomatal conductance (*g<sub>s</sub>*) (Figure 4b) was slightly lower in summer than spring. Midday *g<sub>s</sub>* was significantly lower in both the drought and warming treatments, particularly in summer (*p* < 0.05 for both).

*F<sub>V</sub>/F<sub>M</sub>* (Figure 5a) increased throughout the year in the morning and at midday, in parallel with the seasonal patterns in *A* (Figure 4a). Morning *F<sub>V</sub>/F<sub>M</sub>* was significantly lower in the drought treatment, particularly in winter (*p* < 0.01). Yield (Figure 5b) had similar seasonal patterns as *F<sub>V</sub>/F<sub>M</sub>*, but was slightly lower in autumn than summer in the morning. Midday Yield was significantly lower in the drought and warming treatments, particularly in spring and autumn.

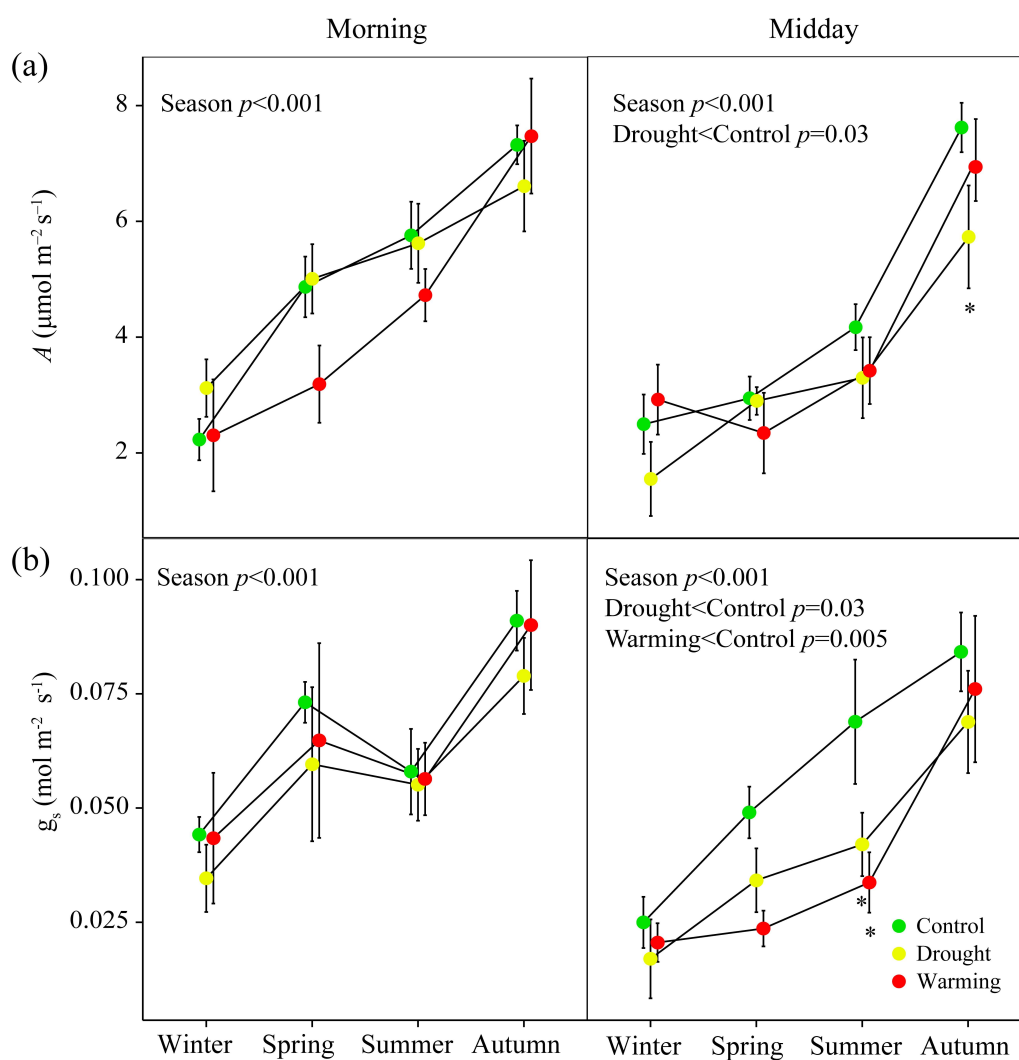


**Figure 4.** Seasonal variation of CO<sub>2</sub> assimilation rate (*A*) (a) and stomatal conductance (*g<sub>s</sub>*) (b) for *Erica multiflora* in 2014. Error bars are standard errors of the mean (*n* = 6 for the drought and warming treatments, and *n* = 12 for the control treatment). The significances of overall repeated-measures ANOVAs are depicted. \* *p* < 0.05 between treatments for each seasonal measurement.

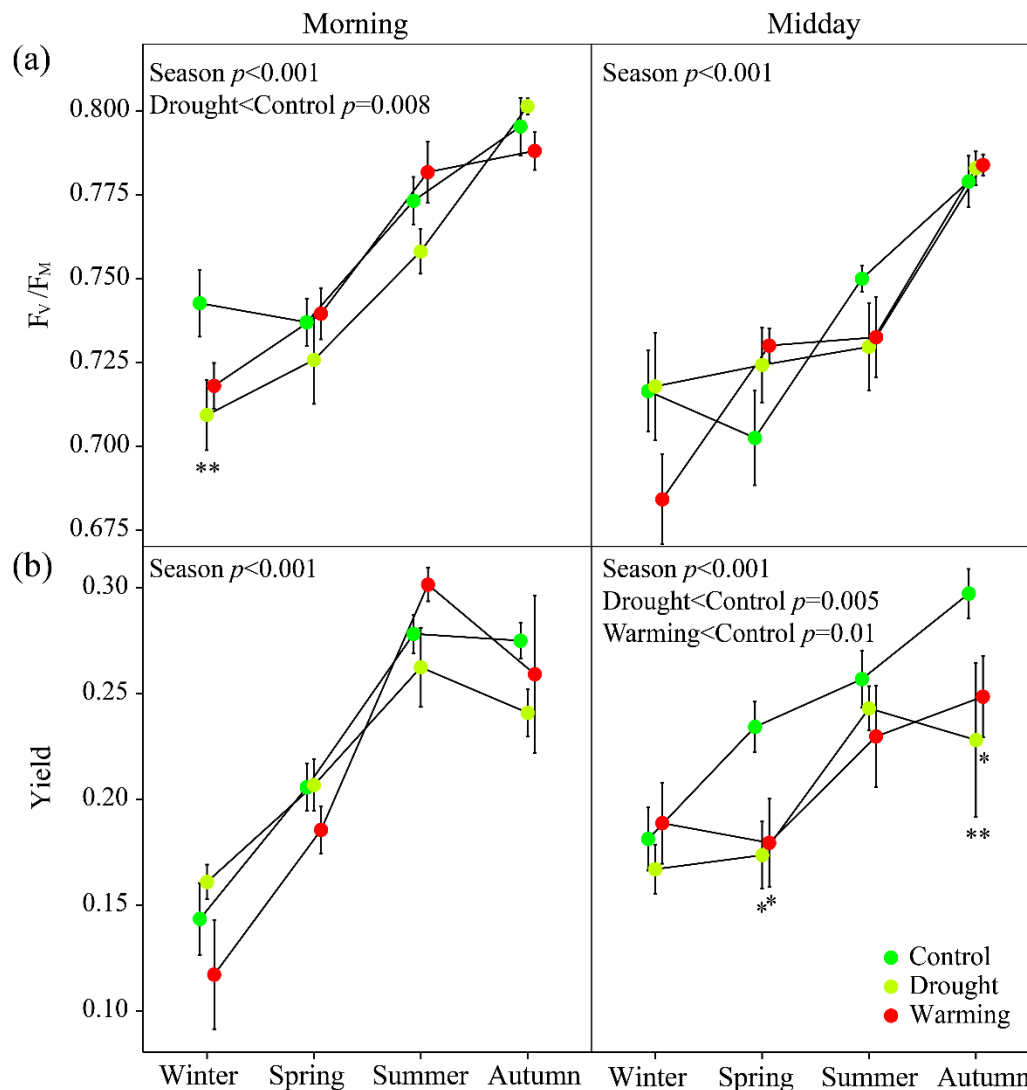


**Figure 5.** Seasonal variation of foliar maximum ( $F_V/F_M$ ) (a) and actual (Yield) (b) photochemical efficiency for *Erica multiflora* in 2014. Error bars are standard errors of the mean ( $n = 6$  for the drought and warming treatments, and  $n = 12$  for the control treatment). The significances of overall repeated-measures ANOVAs are depicted. \*  $p < 0.05$ , \*\*  $p < 0.01$  between treatments for each seasonal measurement.

The seasonality of PRI (Figure 6a) was similar to that of  $A$  and  $F_V/F_M$ . PRI was significantly lower in the warming treatment both in the morning and at midday, particularly in the morning in winter ( $p < 0.05$ ) and at midday in summer ( $p < 0.01$ ). NDVI (Figure 6b) was lowest in spring and similar in winter and summer but did not differ significantly between the treatments, both in the morning and at midday. Interestingly, morning WI (Figure 7) varied similarly to WC (Figure 3) throughout the year. Midday WI, however, was significantly lower in the drought and warming treatments, particularly in summer ( $p < 0.01$  for both) and autumn ( $p < 0.01$  for the warming treatment). NDCI (higher values indicate higher chlorophyll contents) (Figure S1a) was stable from winter to summer but increased rapidly in autumn. NDCI was lower in the warming and drought treatments both in the morning and at midday. SIPI (an estimator of the carotenoids/chlorophyll relationship; higher values indicate higher carotenoid/chlorophyll ratios) (Figure S1b) increased from winter to spring and then decreased to minimum values in autumn.

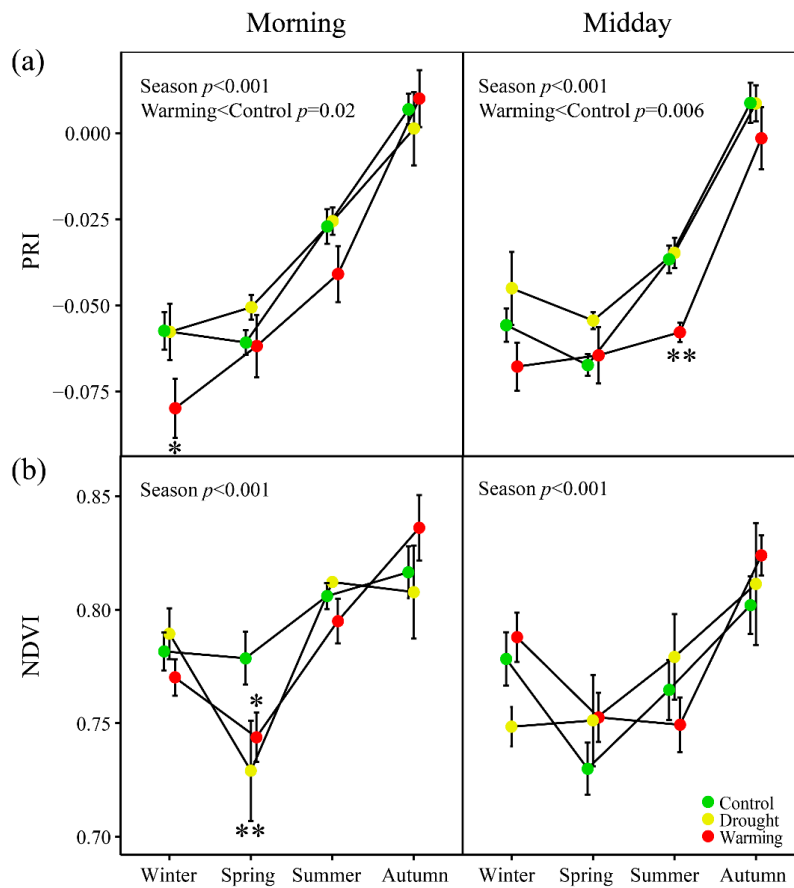


**Figure 6.** Seasonal variation of the photochemical reflectance index (PRI) (a) and normalized difference vegetation index (NDVI) (b) for *Erica multiflora* in 2014. Error bars are standard errors of the mean (n = 6 for the drought and warming treatments, and n = 12 for the control treatment). The significances of overall repeated-measures ANOVAs are depicted. \* p < 0.05, \*\* p < 0.01 between treatments for each seasonal measurement.

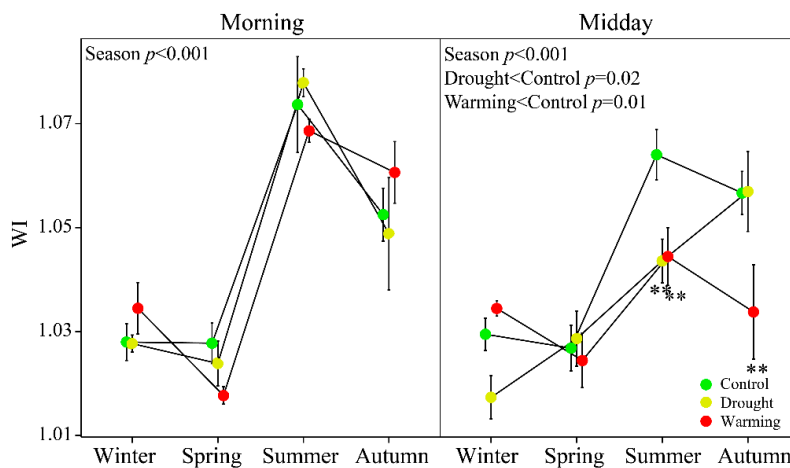


**Figure 7.** Seasonal variation of the water index (WI) for *Erica multiflora* in 2014. Error bars are standard errors of the mean (n = 6 for the drought and warming treatments, and n = 12 for the control treatment). The significances of overall repeated-measures ANOVAs are depicted. \*\* p < 0.01 between treatments for each seasonal measurement.

### 3.3. Relationships of $A$ with PRI, WC, Fluorescence and the Other Vegetation Indices

PRI and  $A$  were significantly correlated in the treatments and over time (Figure 8a). NDVI only poorly tracked the photosynthetic changes (Figure 8b). The indicators of foliar water status, WC (Figure S2a), however, was not correlated with the seasonality of photosynthesis. WI (Figure S2b) was only weakly correlated with  $A$ .  $F_V/F_M$  and Yield had significant relationships with  $A$  (Figure S3) but more weakly than PRI. NDCI also tracked photosynthetic seasonality less well than PRI, with an  $R^2$  range of 0.47–0.94 in the treatments (Figure S4a). SIPI was only weakly correlated with  $A$  (Figure S4b), unlike PRI and NDCI.

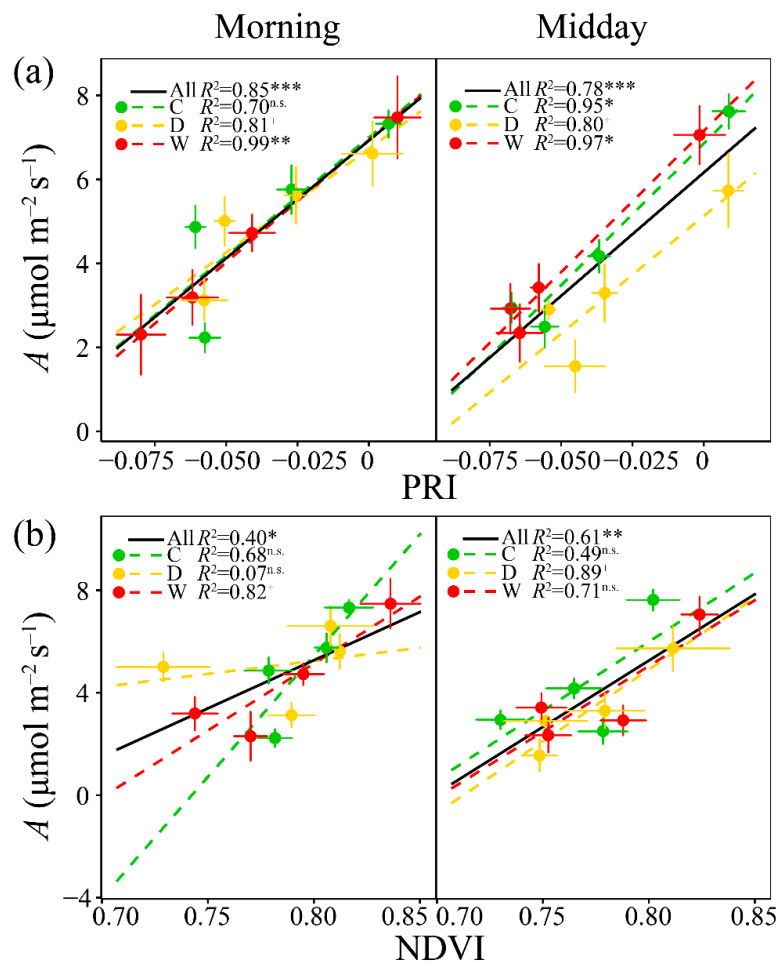


**Figure 8.** Relationships of CO<sub>2</sub> assimilation rate ( $A$ ) with the photochemical reflectance index (PRI) (a) and normalized difference vegetation index (NDVI) (b) for *Erica multiflora* in 2014. The black lines represent the linear relationships over all three treatments. n.s.  $p > 0.1$ , +  $p < 0.1$ , \*  $p < 0.05$ , \*\*  $p < 0.01$  and \*\*\*  $p < 0.001$  between variables. C, D and W indicate the control, drought and warming treatments, respectively.

### 3.4. Relationships between WC and WI

WI accounted for 64% of the variance of WC in the morning, 21% lower than at midday (Figure 9). All the correlations between WI and WC were not significant for treatments with a range of  $R^2$  between 0.49 and 0.74.

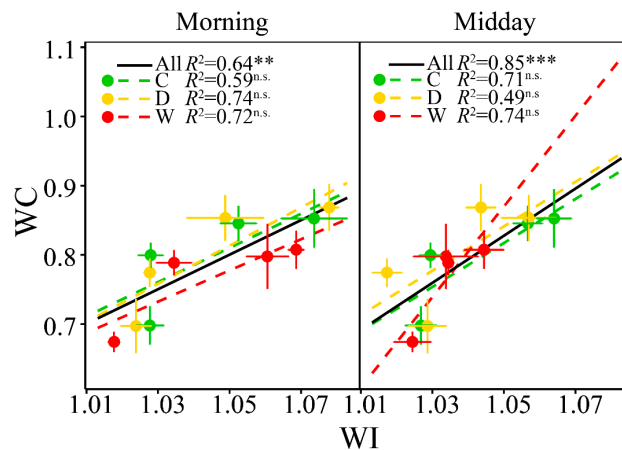


**Figure 9.** Relationships between water content (WC) and the water index (WI) for *Erica multiflora* in 2014. The black lines represent the linear relationships over all three treatments. n.s.  $p > 0.1$ , \*\*  $p < 0.01$  and \*\*\*  $p < 0.001$  between variables. C, D and W indicate the control, drought and warming treatments, respectively.

### 3.5. Relationships of PRI with the Fluorescence Parameters and Indices of Vegetation Pigments

PRI was significantly correlated with  $F_V/F_M$  (Figure 10a,  $R^2$  of 0.94–0.99 in the morning and at midday) in control and drought treatments, but weakly with Yield (Figure 10b). Interestingly, PRI was strongly correlated with NDCI (Figure S5a,  $R^2 > 0.78$ ), particularly in the drought and warming treatment ( $R^2$  was between 0.87 and 0.99). The correlation between PRI and SIPI was also high, with a clearly better relationships at midday (Figure S5b).

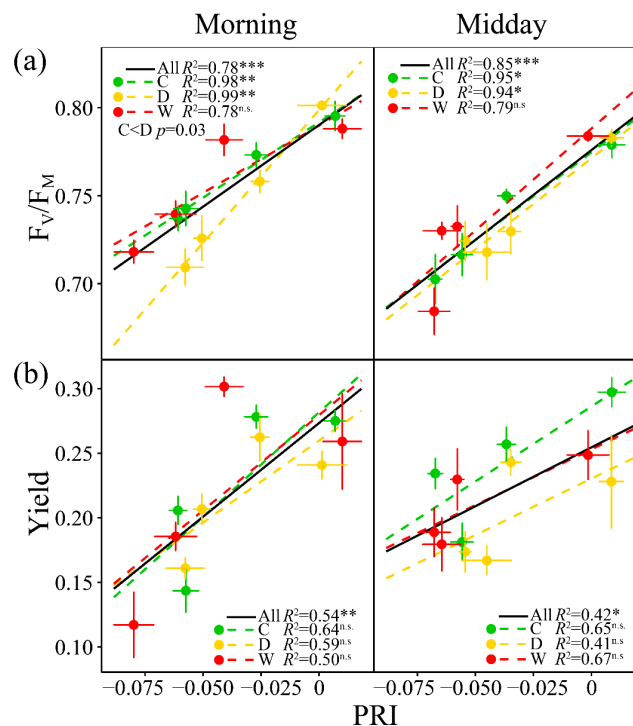


**Figure 10.** Relationships of maximum ( $F_V/F_M$ ) (a) and actual (Yield) (b) photochemical efficiency of PSII with the photochemical reflectance index (PRI) for *Erica multiflora* in 2014. The black lines represent the linear relationships over all three treatments. n.s.  $p > 0.1$ , \*  $p < 0.05$ , \*\*  $p < 0.01$  and \*\*\*  $p < 0.001$  between variables. C, D and W indicate the control, drought and warming treatments, respectively.

### 3.6. Responses of $\Delta$ PRI to $\Delta A$ and $\Delta$ Yield

PRI varied diurnally similarly with  $A$  and Yield in all treatments throughout the year, particularly in the warming treatment (Figure 11).  $\Delta A$ ,  $\Delta$ Yield and  $\Delta$ PRI varied from high winter values (near or  $> 0$ ) to low summer values ( $< 0$ ) and then slightly increased in autumn (Figure 11). These changes indicated that photosynthesis and PRI were mostly lowest at midday in summer.  $\Delta$ Yield (Figure 11b) was significantly higher ( $p < 0.05$ ) in the control than in the drought and warming treatments that had low negative values from spring to autumn, i.e., midday Yield was much lower in the drought and warming treatments.  $\Delta A$  and  $\Delta$ Yield were strongly correlated with  $\Delta$ PRI (Figure 12,  $> 50\%$  of the variability was explained by  $\Delta$ PRI for all treatments combined), particularly for the drought ( $R^2 = 0.82$  and  $p < 0.1$  for  $\Delta A$ ,  $R^2 = 0.95$  and  $p < 0.05$  for  $\Delta$ Yield) and warming ( $R^2 = 0.98$  and  $p < 0.05$  for both) treatments. The slopes of these relationships were not different among treatments except the slope between  $\Delta$ Yield and  $\Delta$ PRI that was lower in the drought than in the warming treatment.

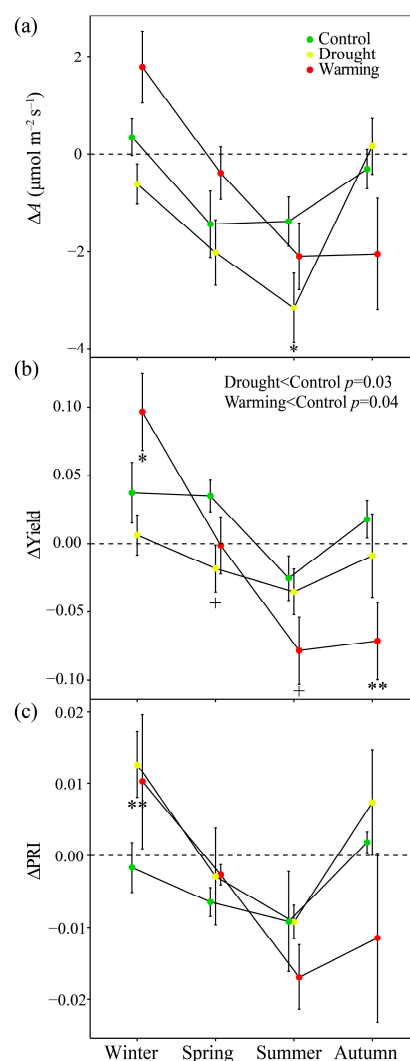


**Figure 11.** Seasonal variation of differential CO<sub>2</sub> assimilation rate ( $\Delta A$ ) (a), actual photochemical efficiency of PSII ( $\Delta$ Yield) (b) and photochemical reflectance index ( $\Delta$ PRI) (c) between midday and early morning measurements for *Erica multiflora* in 2014. Error bars are standard errors of the mean ( $n = 6$  for the drought and warming treatments, and  $n = 12$  for the control treatment). The significances of overall repeated-measures ANOVAs are depicted. +  $p < 0.1$ , \*  $p < 0.05$ , \*\*  $p < 0.01$  between treatments for each seasonal measurement.

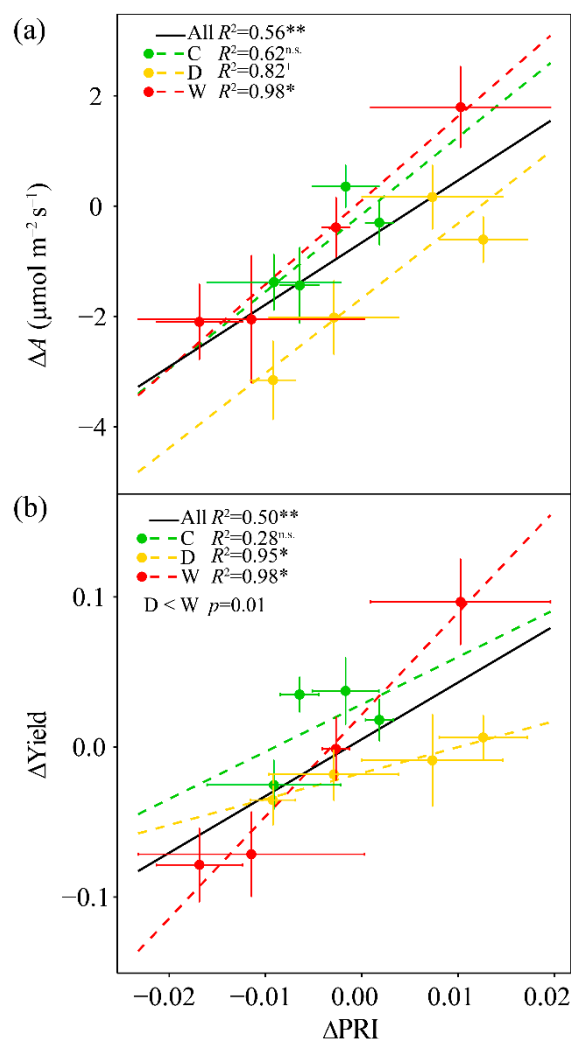


**Figure 12.** Relationships of differential  $\text{CO}_2$  assimilation rate ( $\Delta A$ ) (a) and actual photochemical efficiency of PSII ( $\Delta \text{Yield}$ ) between midday and early morning measurements (b) with the differential photochemical reflectance index ( $\Delta \text{PRI}$ ) (c) for *Erica multiflora* in 2014. The black lines represent the linear relationships over all three treatments. n.s.  $p > 0.1$ , +  $p < 0.1$ , \*  $p < 0.05$  and \*\*  $p < 0.01$  between variables. C, D and W indicate the control, drought and warming treatments, respectively.

#### 4. Discussion

Our results showed that PRI, but not NDVI, efficiently tracked the photosynthetic seasonality of mature evergreen plants under experimental warming and drought conditions. PRI also tracked photosynthetic activity better than NDCI and SIPI. WI was a good indicator of the seasonal variability of foliar WC in this drought-tolerant evergreen shrub. Importantly,  $\Delta \text{PRI}$  detected the midday depression in photosynthesis in response to warming and drought conditions, which are generally accompanied by multiple physiological processes (e.g., lower midday  $g_s$  in this study) and are not readily detectable.

##### 4.1. PRI Assessment of Seasonal Photosynthesis under Long-Term Drought and Warming Conditions

The study site, a typical Mediterranean region, has been generally characterized by low precipitation and high temperatures in previous summers [2] and in future climatic projections [10]. The summer was wetter and the spring was drier in 2014 than in previous years due to a higher summer precipitation (82.1 mm more than in spring) (Figure 1) and a considerably lower spring soil water content (Figure 2a; [18,30]). During summer sampling dates, the measurements were conducted

after several days of rain (Figure 1), so that photosynthetic performance was not representative of common Mediterranean summers. The drier spring in our study year (Figure 1) also led to lower values in CO<sub>2</sub> assimilation rate,  $F_V/F_M$  and Yield compared with summer and autumn (Figure 4a). Thus,  $A$  consequently increased seasonally from winter to autumn, and  $F_V/F_M$  increased from spring to summer, in contrast to the significant decrease in previous studies [28,56]. These seasonal increases in  $A$  and  $F_V/F_M$  were efficiently tracked by PRI, with strong correlations in all treatments (Figure 8a), which were stronger than in previous years in this experimental system [47].

$A$ ,  $g_S$  and Yield at midday, and  $F_V/F_M$  in the morning were significantly lower in the drought treatment than control in some seasons (winter  $F_V/F_M$ , autumn  $A$  and summer  $g_S$ ;  $p < 0.05$ ; Figures 4 and 5a), likely due to the effect of water stress.  $g_S$  and Yield at midday were also lower in the warming treatment than under control conditions ( $p \leq 0.01$ ; Figures 4b and 5b). It has been reported that drought and warming can advance the spring growing season, affect reproductive performance and decrease plant productivity of *E. multiflora* [63,64]. The drier and warmer conditions projected for the future could affect diversity, decrease biomass and increase mortality in Mediterranean ecosystems [11,18,21,65]. Additionally, warmer conditions generally imply that plants need more water due to higher transpiration. The interactive effects of warmer and drier conditions could also have an important effect on plant photosynthetic dynamics and growth in Mediterranean ecosystems. In our study site, the treatment combined warming and drought and should be focused in future studies, since the cross occurrence of warming and drought has been observed under climate change conditions [1,2,5,9].

PRI provided a simple method to non-destructively assess such long-term effects for drought-tolerant plants. NDVI, however, was only weakly correlated with  $A$  (Figure 8b), in contrast to a higher correlation of previous study [47]. NDCI was also strongly seasonally correlated with  $A$  (Figure S4a), and SIPI was weakly and negatively correlated with  $A$  (Figure S4b), but neither was as strongly correlated as PRI. PRI was not only sensitive to long-term carotenoid/chlorophyll changes, but also to short-term xanthophyll pigment conversion [46,50,66]. The strong correlations of PRI with NDCI and SIPI (Figure S5) supported the importance of pigments in using PRI to monitor the photosynthetic apparatus at seasonal timescales [46], because NDCI is an index of chlorophyll changes [51,61] and SIPI is associated with carotenoid and chlorophyll ratios [62]. PRI and NDCI were much lower in the warming than the control treatment, further demonstrating the regulation of de-epoxidation state of the xanthophyll cycle in plants confronted by heat stress, which affected the changes of the photosynthetic pigments. Our results also indicated that these indices were sensitive to decreases in foliar gas exchange and photochemical efficiency induced by warming.

Seasonal changes of the pools of carotenoid pigments, including xanthophyll pigments but also lutein, neoxanthin and  $\beta$ -carotenoid, play an important role in preventing photosynthetic inhibition and downregulation [41,67,68]. A previous study at our site found large seasonal changes of carotenoids in *E. multiflora* [30]. Our study did not find pigment changes, but the strong interactions of the indices associated with pigments (PRI, NDCI and SIPI) and photosynthesis indirectly illustrate the role of the pigments in the seasonality of photosynthetic regulation.

Variations in canopy structure, such as shadows and plant architecture, generally also have large effects on the seasonality of PRI. Filella et al. [47] proposed that PRI could be a better indicator of photosynthetic activity than NDVI, under increased vegetation coverage or LAI during the early successional stages of the *E. multiflora* canopy. Our study supports this proposition, where NDVI was shown to reach near saturation values (Figure 6b), while PRI continued to increase synchronously with CO<sub>2</sub> assimilation rate (Figures 4a and 6a). Additionally, NDVI was insensitive to disturbances in plant functionality following drought or warming. Many reports have demonstrated that NDVI is readily saturated in dense canopies and/or at high LAIs, which could lead to poor or failed assessments of photosynthetic activity and plant biomass [36,37,48].

PRI has also been used to track variability in  $A$  in mature olive trees in response to seasonal water stress [69]. The prolonged summer-drought limited light-use efficiency (LUE) which was assessed by

satellite-based PRI [70]. Our study confirmed the ability of PRI to detect the effects of seasonal water deficits on photosynthesis and demonstrated the potential of PRI to assess the impacts of climatic warming on plant photosynthesis.

#### 4.2. WI Tracked the Seasonal Changes of Foliar WC

Water availability plays a key role in photosynthetic regulation in *E. multiflora* [28]. Many reports have demonstrated that WI can be a non-destructive proxy of plant water content for identifying water stress and predicting crop yield [60,71–73]. Our results also showed that the WI clearly detected changes in WC. However, neither WC nor WI were highly correlated with CO<sub>2</sub> assimilation rate (Figure S2a,b). This decoupling of foliar water status and photosynthesis in *E. multiflora* was probably caused by the large role played by soil water availability in photosynthetic adjustment in Mediterranean ecosystems, which generally encounter drought stress [18,24,26]. In our study, *A* and *g<sub>s</sub>* values in summer were higher than in spring and winter (Figure 4) but SWC values were apparently lower than in all the other seasons (Figure 2a). Such results indicate that summer wetness had no effects on SWC at 10 cm depth in our study site, although our summer measurements were conducted after strong rains only few days before sampling. Our measurement of SWC at 10 cm thus had limitations to explain the physiological and photosynthetic changes in our study site. The measurement of SWC at different depths appears necessary to avoid such limitations.

#### 4.3. PRI Assessment of Midday Depressions of Photosynthesis under Long-Term Drought and Warming

The low negative values of foliar  $\Delta A$  and  $\Delta \text{Yield}$  in summer at the diurnal scale (Figure 11a, b) identified the midday depression of photosynthesis, which has been previously reported for the same site by [56]. The higher winter  $\Delta A$  and  $\Delta \text{Yield}$  in the warming than the control treatment indicated that warming was beneficial to winter photosynthetic activity. In contrast, the lower negative  $\Delta \text{Yield}$  in summer and autumn in the warming than the control treatment demonstrated that warming increased midday depression of Yield in these two seasons. The drought treatment, however, increased spring and summer midday depression of photosynthesis, marginally decreased Yield in spring, and had no effect on winter and autumn photosynthetic depression. These results demonstrate that plant photosynthesis in the summer season was sensitive to warming and drought, and indicate that possible future climate change might enhance photosynthetic midday depression. Interestingly, the patterns of  $\Delta \text{PRI}$  with midday depression of photosynthesis were similar in the warming and drought treatments. These results, together with the strong correlations of  $\Delta \text{PRI}$  with  $\Delta A$  and  $\Delta \text{Yield}$  shown in Figure 12, illustrate that  $\Delta \text{PRI}$  is highly sensitive to midday photoinhibition under experimental warming and that it can be used as an indicator of reduced carbon assimilation.

The midday depression of photosynthesis in Mediterranean summers can be caused to a large extent by the excessive noon irradiance and high temperature [74], which can profoundly influence diurnal PRI patterns and decrease midday PRIs [55]. Short-term changes of PRI have been associated with rapid conversion of xanthophyll pigments that protect the photosystem from photoinhibition at high midday irradiances [34,55] and downregulate PSII photochemical efficiency (Figure 11b; [74]). The regulation of photosynthetic midday depression aids plant survival when environmental conditions are unfavorable but decreases LUE and plant productivity [55]. Models have demonstrated that photosynthetic downregulation reduces carbon uptake and affects the carbon budget [54]. Our study introduces a simple method to detect the photosynthetic midday depression. Gamon and Bond [55] reported that PRI was sensitive to illumination and photosynthetic downregulation in a short-term study, which supports the potential utility of  $\Delta \text{PRI}$  for monitoring the seasonal midday depression of photosynthesis in the present study.

The midday depression of photochemical activity in summer was also due to the significantly lower  $\Delta g_s$  in warming and drought treatments than in control ( $p < 0.05$ ). Lower  $g_s$  in *E. multiflora* generally co-occur with lower transpiration rates and higher vapor-pressure deficits [18,56]. Lower  $g_s$

can also decrease midday transpiration rates and prevent or control the decrease in foliar water potential [25,75], eliciting lower midday rates of carbon assimilation.

He et al. [76] recently demonstrated that MODIS-based PRI was sensitive to LUE constrained by water stress due to low soil water content. Magney et al. [53] also reported that  $\Delta$ PRI was more sensitive to water and nutrient limitation but less sensitive to LAI and chlorophyll content throughout the wheat growing season, which enabled  $\Delta$ PRI to deconvolve the diurnal component from seasonal changes. Together with these previous reports, our study further supported the ability of  $\Delta$ PRI to detect the responses of photosynthetic midday depression to environmental stresses.

## 5. Conclusions and Final Remarks

In our study, we used PRI to detect the seasonality of photosynthesis in *E. multiflora* under long-term drought and warming conditions. WI also provided a simple method for non-destructively detecting changes in plant water content in this drought-tolerant shrub. Our study also indicated that warming was beneficial to winter photosynthetic activity, and that warming and drought increased summer midday depression of photosynthesis for semi-arid Mediterranean evergreen shrub.  $\Delta$ PRI provided a simple method for detecting this midday depression or downregulation of photosynthesis response to climate change.

It should be noted that we measured photosynthesis under constant light conditions that can represent LUE at a given light intensity. Further study should test the utility of PRI and  $\Delta$ PRI as indicators of plant photosynthetic dynamics and midday depression under natural illumination in evergreen shrubs and other functional types. Importantly, assessments of PRI should be adjusted based on the effects of canopy structure, pigments, view angle and irradiance etc. [52,53,70,77,78], to facilitate its applicability in interpreting photosynthetic activity and in the large-scale monitoring of carbon uptake. Increasingly used unmanned aerial vehicles (UAVs) with various optical sensors provide an exciting opportunity to monitor multiple optical signals (e.g., PRI and WI) with high spatiotemporal resolution [79]. MODIS (Moderate Resolution Imaging Spectroradiometer) aboard the Terra and Aqua satellites provides the possibility of retrieving PRI or CCI (chlorophyll/carotenoid index, [41]) both in the morning and at midday, which can be further applied to test the diurnal changes of PRI or CCI and the utility of assessing carbon budget under ongoing and future climate change at larger spatial and longer temporal scales. GOME-2 (Global Ozone Monitoring Experiment-2) spectrometer, aboard the Metop satellite with a high spectral (0.2–0.4 nm in ultraviolet and visible spectrum) and temporal resolution (enables scanning the earth surface within 1.5 day), also provides the possibility of calculation of PRI to detect changes in carbon uptake at high spatiotemporal scales.

Our ground-based study could provide basic information for validating the airborne or satellite-based inferences of photosynthesis using PRI in response to environmental stresses and the ongoing changes to climate, particularly, in regions dominated by evergreen species where photosynthetic capacity is mainly constrained by stomatal adjustment and water availability, both in soil and leaves, due to the effects of summer drought and low precipitation, such as our study site. Remotely sensing pigment activity to assess the seasonality of photosynthesis is a basic but vital step toward the ultimate assessment of the global carbon budget.

**Supplementary Materials:** The following are available online at [www.mdpi.com/2072-4292/9/11/1189/s1](http://www.mdpi.com/2072-4292/9/11/1189/s1). Figure S1. Seasonal variation of the normalized difference chlorophyll index (NDCI) (a) and the structure-independent pigment index (SIPI) (b) for *Erica multiflora* in 2014. Figure S2. Relationships of CO<sub>2</sub> assimilation rate (A) with water content (WC) (a) and the water index (WI) (b) for *Erica multiflora* in 2014. Figure S3. Relationships of CO<sub>2</sub> assimilation rate (A) with maximum ( $F_V/F_M$ ) (a) and actual (Yield) (b) photochemical efficiency of PSII for *Erica multiflora* in 2014. Figure S4. Relationships of CO<sub>2</sub> assimilation rate (A) with the normalized difference chlorophyll index (NDCI) (a) and the structure-independent pigment index (SIPI) (b) for *Erica multiflora* in 2014. Figure S5. Relationships of the normalized difference chlorophyll index (NDCI) (a) and the structure-independent pigment index (SIPI) (b) with the photochemical reflectance index (PRI) for *Erica multiflora* in 2014.

**Acknowledgments:** This work was supported by the Spanish Government project CGL2016-79835-P, the European Research Council Synergy grant SyG-2013-610028 IMBALANCE-P, and the Catalan Government project SGR 2014-274. Chao Zhang gratefully acknowledges the support from the Chinese Scholarship Council.

**Author Contributions:** J.P. and I.F. conceived and designed the experiments; C.Z., D.L., R.O., J.L., and D.A. performed the experiments; C.Z. and I.F. analyzed the data; C.Z. wrote the main manuscript, and all the authors contributed to write and discuss the paper.

**Conflicts of Interest:** The authors declare no conflict of interest.

## References

1. Dai, A. Drought under global warming: A review. *Wiley Interdiscip. Rev. Clim. Chang.* **2011**, *2*, 45–65. [[CrossRef](#)]
2. Vicente-Serrano, S.M.; Lopez-Moreno, J.-I.; Beguería, S.; Lorenzo-Lacruz, J.; Sanchez-Lorenzo, A.; García-Ruiz, J.M.; Azorin-Molina, C.; Morán-Tejeda, E.; Revuelto, J.; Trigo, R.; et al. Evidence of increasing drought severity caused by temperature rise in southern Europe. *Environ. Res. Lett.* **2014**, *9*, 44001. [[CrossRef](#)]
3. Sheffield, J.; Wood, E.F.; Roderick, M.L. Little change in global drought over the past 60 years. *Nature* **2012**, *491*, 435–438. [[CrossRef](#)] [[PubMed](#)]
4. Ciais, P.; Reichstein, M.; Viovy, N.; Granier, A.; Ogée, J.; Allard, V.; Aubinet, M.; Buchmann, N.; Bernhofer, C.; Carrara, A.; et al. Europe-wide reduction in primary productivity caused by the heat and drought in 2003. *Nature* **2005**, *437*, 529–533. [[CrossRef](#)] [[PubMed](#)]
5. Yuan, W.; Cai, W.; Chen, Y.; Liu, S.S.; Dong, W.; Zhang, H.; Yu, G.; Chen, Z.; He, H.; Guo, W.; et al. Severe summer heatwave and drought strongly reduced carbon uptake in Southern China. *Sci. Rep.* **2016**, *6*, 18813. [[CrossRef](#)] [[PubMed](#)]
6. Bertrand, R.; Riofrío-Dillon, G.; Lenoir, J.; Drapier, J.; de Ruffray, P.; Gégout, J.-C.; Loreau, M. Ecological constraints increase the climatic debt in forests. *Nat. Commun.* **2016**, *7*, 12643. [[CrossRef](#)] [[PubMed](#)]
7. Carnicer, J.; Coll, M.; Ninyerola, M.; Pons, X.; Sánchez, G.; Peñuelas, J. Widespread crown condition decline, food web disruption, and amplified tree mortality with increased climate change-type drought. *Proc. Natl. Acad. Sci. USA* **2011**, *108*, 1474–1478. [[CrossRef](#)] [[PubMed](#)]
8. McDowell, N.; Pockman, W.T.; Allen, C.D.; Breshears, D.D.; Cobb, N.; Kolb, T.; Plaut, J.; Sperry, J.; West, A.; Williams, D.G.; et al. Mechanisms of plant survival and mortality during drought: Why do some plants survive while others succumb to drought? *New Phytol.* **2008**, *178*, 719–739. [[CrossRef](#)] [[PubMed](#)]
9. Sheffield, J.; Wood, E.F. Projected changes in drought occurrence under future global warming from multi-model, multi-scenario, IPCC AR4 simulations. *Clim. Dyn.* **2008**, *31*, 79–105. [[CrossRef](#)]
10. Giorgi, F.; Lionello, P. Climate change projections for the Mediterranean region. *Glob. Planet. Chang.* **2008**, *63*, 90–104. [[CrossRef](#)]
11. Nardini, A.; Lo Gullo, M.A.; Trifilò, P.; Salleo, S. The challenge of the Mediterranean climate to plant hydraulics: Responses and adaptations. *Environ. Exp. Bot.* **2014**, *103*, 68–79. [[CrossRef](#)]
12. Peñuelas, J.; Sardans, J.; Estiarte, M.; Ogaya, R.; Carnicer, J.; Coll, M.; Barbeta, A.; Rivas-Ubach, A.; Llusà, J.; Garbulsky, M.; et al. Evidence of current impact of climate change on life: A walk from genes to the biosphere. *Glob. Chang. Biol.* **2013**, *19*, 2303–2338. [[CrossRef](#)] [[PubMed](#)]
13. Peñuelas, J.; Sardans, J.; Filella, I.; Estiarte, M.; Llusà, J.; Ogaya, R.; Carnicer, J.; Bartrons, M.; Rivas-Ubach, A.; Grau, O.; et al. Assessment of the impacts of climate change on Mediterranean terrestrial ecosystems based on data from field experiments and long-term monitored field gradients in Catalonia. *Environ. Exp. Bot.* **2017**. [[CrossRef](#)]
14. Cook, B.I.; Anchukaitis, K.J.; Touchan, R.; Meko, D.M.; Cook, E.R. Spatiotemporal drought variability in the Mediterranean over the last 900 years. *J. Geophys. Res. Atmos.* **2016**, *121*, 2060–2074. [[CrossRef](#)]
15. Martín Vide, J. *Tercer Informe Sobre El Canvi Climàtic a Catalunya*; Generalitat de Catalunya i Institut d'Estudis Catalans: Barcelona, Spain, 2016.
16. Liu, D.; Estiarte, M.; Ogaya, R.; Yang, X.; Peñuelas, J. Shift in community structure in an early-successional Mediterranean shrubland driven by long-term experimental warming and drought and natural extreme droughts. *Glob. Chang. Biol.* **2017**, *23*, 4267–4279. [[CrossRef](#)] [[PubMed](#)]

17. Klein, T.; Shpringer, I.; Fikler, B.; Elbaz, G.; Cohen, S.; Yakir, D. Relationships between stomatal regulation, water-use, and water-use efficiency of two coexisting key Mediterranean tree species. *For. Ecol. Manag.* **2013**, *302*, 34–42. [[CrossRef](#)]
18. Liu, D.; Llusia, J.; Ogaya, R.; Estiarte, M.; Llorens, L.; Yang, X.; Peñuelas, J. Physiological adjustments of a Mediterranean shrub to long-term experimental warming and drought treatments. *Plant Sci.* **2016**, *252*, 53–61. [[CrossRef](#)] [[PubMed](#)]
19. Wu, Z.; Dijkstra, P.; Koch, G.W.; Peñuelas, J.; Hungate, B.A. Responses of terrestrial ecosystems to temperature and precipitation change: A meta-analysis of experimental manipulation. *Glob. Chang. Biol.* **2011**, *17*, 927–942. [[CrossRef](#)]
20. Barbeta, A.; Ogaya, R.; Peñuelas, J. Dampening effects of long-term experimental drought on growth and mortality rates of a Holm oak forest. *Glob. Chang. Biol.* **2013**, *19*, 3133–3144. [[CrossRef](#)] [[PubMed](#)]
21. Liu, D.; Ogaya, R.; Barbeta, A.; Yang, X.; Peñuelas, J. Contrasting impacts of continuous moderate drought and episodic severe droughts on the aboveground-biomass increment and litterfall of three coexisting Mediterranean woody species. *Glob. Chang. Biol.* **2015**, *21*, 4196–4209. [[CrossRef](#)] [[PubMed](#)]
22. Helman, D.; Osem, Y.; Yakir, D.; Lensky, I.M. Relationships between climate, topography, water use and productivity in two key Mediterranean forest types with different water-use strategies. *Agric. For. Meteorol.* **2017**, *232*, 319–330. [[CrossRef](#)]
23. Powell, T.L.; Galbraith, D.R.; Christoffersen, B.O.; Harper, A.; Imbuzeiro, H.M.A.; Rowland, L.; Almeida, S.; Brando, P.M.; da Costa, A.C.L.; Costa, M.H.; et al. Confronting model predictions of carbon fluxes with measurements of Amazon forests subjected to experimental drought. *New Phytol.* **2013**, *200*, 350–365. [[CrossRef](#)] [[PubMed](#)]
24. Asensio, D.; Peñuelas, J.; Ogaya, R.; Llusia, J. Seasonal soil and leaf CO<sub>2</sub> exchange rates in a Mediterranean holm oak forest and their responses to drought conditions. *Atmos. Environ.* **2007**, *41*, 2447–2455. [[CrossRef](#)]
25. Farquhar, G.D.; Sharkey, T.D. Stomatal conductance and photosynthesis. *Annu. Rev. Plant Physiol.* **1982**, *33*, 317–345. [[CrossRef](#)]
26. Ogaya, R.; Llusia, J.; Barbeta, A.; Asensio, D.; Liu, D.; Alessio, G.A.; Peñuelas, J. Foliar CO<sub>2</sub> in a holm oak forest subjected to 15 years of climate change simulation. *Plant Sci.* **2014**, *226*, 101–107. [[CrossRef](#)] [[PubMed](#)]
27. Crafts-Brandner, S.J.; Salvucci, M.E. Rubisco activase constrains the photosynthetic potential of leaves at high temperature and CO<sub>2</sub>. *Proc. Natl. Acad. Sci. USA* **2000**, *97*, 13430–13435. [[CrossRef](#)] [[PubMed](#)]
28. Llorens, L.; Peñuelas, J.; Filella, I. Diurnal and seasonal variations in the photosynthetic performance and water relations of two co-occurring Mediterranean shrubs, *Erica multiflora* and *Globularia alypum*. *Physiol. Plant.* **2003**, *118*, 84–95. [[CrossRef](#)] [[PubMed](#)]
29. Gallé, A.; Haldimann, P.; Feller, U. Photosynthetic performance and water relations in young pubescent oak (*Quercus pubescens*) trees during drought stress and recovery. *New Phytol.* **2007**, *174*, 799–810. [[CrossRef](#)] [[PubMed](#)]
30. Nogués, I.; Peñuelas, J.; Llusia, J.; Estiarte, M.; Munné-Bosch, S.; Sardans, J.; Loreto, F. Physiological and antioxidant responses of *Erica multiflora* to drought and warming through different seasons. *Plant Ecol.* **2012**, *213*, 649–661. [[CrossRef](#)]
31. Demmig-Adams, B.; Adams, W.W. Photoprotection in an ecological context: The remarkable complexity of thermal energy dissipation. *New Phytol.* **2006**, *172*, 11–21. [[CrossRef](#)] [[PubMed](#)]
32. Porcar-Castell, A.; Tyystjärvi, E.; Atherton, J.; Van Der Tol, C.; Flexas, J.; Pfündel, E.E.; Moreno, J.; Frankenberg, C.; Berry, J.A. Linking chlorophyll a fluorescence to photosynthesis for remote sensing applications: Mechanisms and challenges. *J. Exp. Bot.* **2014**, *65*, 4065–4095. [[CrossRef](#)] [[PubMed](#)]
33. Gamon, J.A.; Peñuelas, J.; Field, C. A narrow-waveband spectral index that tracks diurnal changes in photosynthetic efficiency. *Remote Sens. Environ.* **1992**, *41*, 35–44. [[CrossRef](#)]
34. Peñuelas, J.; Filella, I.; Gamon, J.A. Assessment of photosynthetic radiation use efficiency with spectral reflectance. *New Phytol.* **1995**, *131*, 291–296. [[CrossRef](#)]
35. Garbulsky, M.F.; Peñuelas, J.; Gamon, J.; Inoue, Y.; Filella, I. The photochemical reflectance index (PRI) and the remote sensing of leaf, canopy and ecosystem radiation use efficiencies. A review and meta-analysis. *Remote Sens. Environ.* **2011**, *115*, 281–297. [[CrossRef](#)]
36. Peñuelas, J.; Garbulsky, M.F.; Filella, I. Photochemical reflectance index (PRI) and remote sensing of plant CO<sub>2</sub> uptake. *New Phytol.* **2011**, *191*, 596–599. [[CrossRef](#)] [[PubMed](#)]

37. Stylinski, C.D.; Gamon, J.A.; Oechel, W.C. Seasonal patterns of reflectance indices, carotenoid pigments and photosynthesis of evergreen chaparral species. *Oecologia* **2002**, *131*, 366–374. [[CrossRef](#)] [[PubMed](#)]
38. Zhang, C.; Filella, I.; Garbulsy, M.; Peñuelas, J. Affecting factors and recent improvements of the photochemical reflectance index (PRI) for remotely sensing foliar, canopy and ecosystemic radiation-use efficiencies. *Remote Sens.* **2016**, *8*, 677. [[CrossRef](#)]
39. Wong, C.Y.S.; Gamon, J.A. Three causes of variation in the photochemical reflectance index (PRI) in evergreen conifers. *New Phytol.* **2015**, *206*, 187–195. [[CrossRef](#)] [[PubMed](#)]
40. Wong, C.Y.S.; Gamon, J.A. The photochemical reflectance index provides an optical indicator of spring photosynthetic activation in evergreen conifers. *New Phytol.* **2015**, *206*, 196–208. [[CrossRef](#)] [[PubMed](#)]
41. Gamon, J.A.; Huemmrich, K.F.; Wong, C.Y.S.; Ensminger, I.; Garrity, S.; Hollinger, D.Y.; Noormets, A.; Peñuelas, J. A remotely sensed pigment index reveals photosynthetic phenology in evergreen conifers. *Proc. Natl. Acad. Sci. USA* **2016**, *113*, 13087–13092. [[CrossRef](#)] [[PubMed](#)]
42. Goerner, A.; Reichstein, M.; Rambal, S. Tracking seasonal drought effects on ecosystem light use efficiency with satellite-based PRI in a Mediterranean forest. *Remote Sens. Environ.* **2009**, *113*, 1101–1111. [[CrossRef](#)]
43. Vicca, S.; Balzarolo, M.; Filella, I.; Granier, A.; Herbst, M.; Knohl, A.; Longdoz, B.; Mund, M.; Nagy, Z.; Pintér, K.; et al. Remotely-sensed detection of effects of extreme droughts on gross primary production. *Sci. Rep.* **2016**, *6*, 1–13. [[CrossRef](#)] [[PubMed](#)]
44. Ripullone, F.; Rivelli, A.R.; Baraldi, R.; Guarini, R.; Guerrieri, R.; Magnani, F.; Peñuelas, J.; Raddi, S.; Borghetti, M. Effectiveness of the photochemical reflectance index to track photosynthetic activity over a range of forest tree species and plant water statuses. *Funct. Plant Biol.* **2011**, *38*, 177–186. [[CrossRef](#)]
45. Rossini, M.; Fava, F.; Cogliati, S.; Meroni, M.; Marchesi, A.; Panigada, C.; Giardino, C.; Busetto, L.; Migliavacca, M.; Amaducci, S.; et al. Assessing canopy PRI from airborne imagery to map water stress in maize. *ISPRS J. Photogramm. Remote Sens.* **2013**, *86*, 168–177. [[CrossRef](#)]
46. Filella, I.; Porcar-Castell, A.; Munné-Bosch, S.; Bäck, J.; Garbulsy, M.F.; Peñuelas, J. PRI assessment of long-term changes in carotenoids/chlorophyll ratio and short-term changes in de-epoxidation state of the xanthophyll cycle. *Int. J. Remote Sens.* **2009**, *30*, 4443–4455. [[CrossRef](#)]
47. Filella, I.; Peñuelas, J.; Llorens, L.; Estiarte, M. Reflectance assessment of seasonal and annual changes in biomass and CO<sub>2</sub> uptake of a Mediterranean shrubland submitted to experimental warming and drought. *Remote Sens. Environ.* **2004**, *90*, 308–318. [[CrossRef](#)]
48. Mänd, P.; Hallik, L.; Peñuelas, J.; Nilson, T.; Duce, P.; Emmett, B.A.; Beier, C.; Estiarte, M.; Garadnai, J.; Kalapos, T.; et al. Responses of the reflectance indices PRI and NDVI to experimental warming and drought in European shrublands along a north-south climatic gradient. *Remote Sens. Environ.* **2010**, *114*, 626–636. [[CrossRef](#)]
49. Zhang, C.; Preece, C.; Filella, I.; Farré-Armengol, G.; Peñuelas, J. Assessment of the response of photosynthetic activity of Mediterranean evergreen oaks to enhanced drought stress and recovery by using PRI and R690/R630. *Forests* **2017**, *8*, 386. [[CrossRef](#)]
50. Gamon, J.A.; Berry, J.A. Facultative and constitutive pigment effects on the photochemical reflectance index (PRI) in sun and shade conifer needles. *Isr. J. Plant Sci.* **2012**, *60*, 85–95. [[CrossRef](#)]
51. Gamon, J.A.; Surfus, J.S. Assessing leaf pigment content and activity with a reflectometer. *New Phytol.* **1999**, *143*, 105–117. [[CrossRef](#)]
52. Soudani, K.; Hmimina, G.; Dufrêne, E.; Berveiller, D.; Delpierre, N.; Ourcival, J.M.; Rambal, S.; Joffre, R. Relationships between photochemical reflectance index and light-use efficiency in deciduous and evergreen broadleaf forests. *Remote Sens. Environ.* **2014**, *144*, 73–84. [[CrossRef](#)]
53. Magney, T.S.; Vierling, L.A.; Eitel, J.U.H.; Huggins, D.R.; Garrity, S.R. Response of high frequency Photochemical Reflectance Index (PRI) measurements to environmental conditions in wheat. *Remote Sens. Environ.* **2016**, *173*, 84–97. [[CrossRef](#)]
54. Arora, V.K.; Boer, G.J.; Christian, J.R.; Curry, C.L.; Denman, K.L.; Zahariev, K.; Flato, G.M.; Scinocca, J.F.; Merryfield, W.J.; Lee, W.G. The effect of terrestrial photosynthesis down regulation on the twentieth-century carbon budget simulated with the CCCma Earth System Model. *J. Clim.* **2009**, *22*, 6066–6088. [[CrossRef](#)]
55. Gamon, J.A.; Bond, B. Effects of irradiance and photosynthetic downregulation on the photochemical reflectance index in Douglas-fir and ponderosa pine. *Remote Sens. Environ.* **2013**, *135*, 141–149. [[CrossRef](#)]

56. Llorens, L.; Peñuelas, J.; Estiearte, M. Ecophysiological responses of two Mediterranean shrubs, *Erica multiflora* and *Globularia alypum*, to experimentally drier and warmer conditions. *Physiol. Plant.* **2003**, *119*, 231–243. [[CrossRef](#)]
57. Peñuelas, J.; Prieto, P.; Beier, C.; Cesaraccio, C.; de Angelis, P.; de Dato, G.; Emmett, B.A.; Estiarte, M.; Garadnai, J.; Gorissen, A.; et al. Response of plant species richness and primary productivity in shrublands along a north-south gradient in Europe to seven years of experimental warming and drought: Reductions in primary productivity in the heat and drought year of 2003. *Glob. Chang. Biol.* **2007**, *13*, 2563–2581. [[CrossRef](#)]
58. Asensio, D.; Peñuelas, J.; Prieto, P.; Estiarte, M.; Filella, I.; Llusià, J. Interannual and seasonal changes in the soil exchange rates of monoterpenes and other VOCs in a Mediterranean shrubland. *Eur. J. Soil Sci.* **2008**, *59*, 878–891. [[CrossRef](#)]
59. Tucker, C.J. Red and photographic infrared linear combinations for monitoring vegetation. *Remote Sens. Environ.* **1979**, *8*, 127–150. [[CrossRef](#)]
60. Peñuelas, J.; Filella, I.; Biel, C.; Serrano, L.; Savé, R. The reflectance at the 950–970 nm region as an indicator of plant water status. *Int. J. Remote Sens.* **1993**, *14*, 1887–1905. [[CrossRef](#)]
61. Gitelson, A.; Merzlyak, M.N. Spectral reflectance changes associated with autumn senescence of *Aesculus hippocastanum* L. and *Acer platanoides* L. leaves. Spectral features and relation to chlorophyll estimation. *J. Plant Physiol.* **1994**, *143*, 286–292. [[CrossRef](#)]
62. Peñuelas, J.; Baret, F.; Filella, I. Semiempirical Indexes to Assess Carotenoids Chlorophyll-a Ratio from Leaf Spectral Reflectance. *Photosynthetica* **1995**, *31*, 221–230.
63. Del Cacho, M.; Peñuelas, J.; Lloret, F.; Peñuelas, J.; Lloret, F. Reproductive output in Mediterranean shrubs under climate change experimentally induced by drought and warming. *Perspect. Plant Ecol. Evol. Syst.* **2013**, *15*, 319–327. [[CrossRef](#)]
64. Prieto, P.; Peñuelas, J.; Niinemets, Ü.; Ogaya, R.; Schmidt, I.K.; Beier, C.; Tietema, A.; Sowerby, A.; Emmett, B.A.; Láng, E.K.; et al. Changes in the onset of spring growth in shrubland species in response to experimental warming along a north-south gradient in Europe. *Glob. Ecol. Biogeogr.* **2009**, *18*, 473–484. [[CrossRef](#)]
65. Prieto, P.; Peñuelas, J.; Lloret, F.; Llorens, L.; Estiarte, M. Experimental drought and warming decrease diversity and slow down post-fire succession in a Mediterranean shrubland. *Ecography* **2009**, *32*, 623–636. [[CrossRef](#)]
66. Porcar-Castell, A.; Garcia-Plazaola, J.I.; Nichol, C.J.; Kolari, P.; Olascoaga, B.; Kuusinen, N.; Fernández-Marín, B.; Pulkkinen, M.; Juurola, E.; Nikinmaa, E. Physiology of the seasonal relationship between the photochemical reflectance index and photosynthetic light use efficiency. *Oecologia* **2012**, *170*, 313–323. [[CrossRef](#)] [[PubMed](#)]
67. Demmig-Adams, B.; Adams, W.W. The role of xanthophyll cycle carotenoids in the protection of photosynthesis. *Trends Plant Sci.* **1996**, *1*, 21–26. [[CrossRef](#)]
68. Niyogi, K. Photoprotection Revisited: Genetic and Molecular Approaches. *Annu. Rev. Plant. Physiol. Plant. Mol. Biol.* **1999**, *50*, 333–359. [[CrossRef](#)] [[PubMed](#)]
69. Marino, G.; Pallozzi, E.; Coccozza, C.; Tognetti, R.; Giovannelli, A.; Cantini, C.; Centritto, M. Assessing gas exchange, sap flow and water relations using tree canopy spectral reflectance indices in irrigated and rainfed *Olea europaea* L. *Environ. Exp. Bot.* **2014**, *99*, 43–52. [[CrossRef](#)]
70. Moreno, A.; Maselli, F.; Gilabert, M.A.; Chiesi, M.; Martínez, B.; Seufert, G. Assessment of MODIS imagery to track light-use efficiency in a water-limited Mediterranean pine forest. *Remote Sens. Environ.* **2012**, *123*, 359–367. [[CrossRef](#)]
71. Claudio, H.C.; Cheng, Y.; Fuentes, D.A.; Gamon, J.A.; Luo, H.; Oechel, W.; Qiu, H.L.; Rahman, A.F.; Sims, D.A. Monitoring drought effects on vegetation water content and fluxes in chaparral with the 970 nm water band index. *Remote Sens. Environ.* **2006**, *103*, 304–311. [[CrossRef](#)]
72. Peñuelas, J.; Pinol, J.; Ogaya, R.; Filella, I. Estimation of plant water concentration by the reflectance Water Index WI (R900/R970). *Int. J. Remote Sens.* **1997**, *18*, 2869–2875. [[CrossRef](#)]
73. Peñuelas, J.; Inoue, Y. Reflectance indices indicative of changes in water and pigment contents of peanut and wheat leaves. *Photosynthetica* **1999**, *36*, 355–360. [[CrossRef](#)]
74. Damesin, C.; Rambal, S. Field-study of leaf photosynthetic performance by a Mediterranean deciduous oak tree (*Quercus pubescens*) during a severe summer drought. *New Phytol.* **1995**, *131*, 159–167.

75. Van der Molen, M.K.; Dolman, A.J.; Ciais, P.; Eglin, T.; Gobron, N.; Law, B.E.; Meir, P.; Peters, W.; Phillips, O.L.; Reichstein, M.; et al. Drought and ecosystem carbon cycling. *Agric. For. Meteorol.* **2011**, *151*, 765–773. [[CrossRef](#)]
76. He, M.; Kimball, J.S.; Running, S.; Ballantyne, A.; Guan, K.; Huemmrich, F. Satellite detection of soil moisture related water stress impacts on ecosystem productivity using the MODIS-based photochemical reflectance index. *Remote Sens. Environ.* **2016**, *186*, 173–183. [[CrossRef](#)]
77. Damm, A.; Guanter, L.; Verhoef, W.; Schläpfer, D.; Garbari, S.; Schaepman, M.E. Impact of varying irradiance on vegetation indices and chlorophyll fluorescence derived from spectroscopy data. *Remote Sens. Environ.* **2015**, *156*, 202–215. [[CrossRef](#)]
78. Hilker, T.; Hall, F.G.; Coops, N.C.; Lyapustin, A.; Wang, Y.; Nesic, Z.; Grant, N.; Black, T.A.; Wulder, M.A.; Kljun, N.; et al. Remote sensing of photosynthetic light-use efficiency across two forested biomes: Spatial scaling. *Remote Sens. Environ.* **2010**, *114*, 2863–2874. [[CrossRef](#)]
79. Gago, J.; Douthe, C.; Coopman, R.E.; Gallego, P.P.; Ribas-Carbo, M.; Flexas, J.; Escalona, J.; Medrano, H. UAVs challenge to assess water stress for sustainable agriculture. *Agric. Water Manag.* **2015**, *153*, 9–19. [[CrossRef](#)]



© 2017 by the authors. Licensee MDPI, Basel, Switzerland. This article is an open access article distributed under the terms and conditions of the Creative Commons Attribution (CC BY) license (<http://creativecommons.org/licenses/by/4.0/>).